

Supporting Information (SI)

Indole-BODIPY: A “turn-on” chemosensor for Hg²⁺ with application in Live Cell imaging

Navdeep Kaur,^a Paramjit Kaur,^{*a} Gaurav Bhatia^b, Kamaljit Singh^{*a} and Jatinder Singh^b

^aDepartment of Chemistry, UGC-Centre of Advanced Studies-II, ^bDepartment of Molecular Biology and Biochemistry, Guru Nanak Dev University, Amritsar-143 005, Punjab, India.

E-mail: paramjit19in@yahoo.co.in; kamaljit19in@yahoo.co.in

1. ¹ H NMR spectrum of 1 in CDCl ₃ .	S1
2. ¹³ C NMR spectrum of 1 in CDCl ₃ .	S2
3. IR spectrum of 1 .	S3
4. Mass spectrum of 1 .	S3
5. HSQC spectrum of 1 in CDCl ₃ .	S4-S5
6. The emission spectral pattern of 1 upon pH titrations with HCl and NaOH in CH ₃ CN.	S5
7. Changes in the emission properties of 1 at 610 nm upon addition of various metal ions.	S6
8. Responsiveness of 1 in the presence of 6.6 equiv. of Hg ²⁺ .	S6
9. Increase in the emission intensity at 612 nm of 1 upon addition of increasing amount of Hg ²⁺ Inset: Graph depicting 3.3 x 10 ⁻⁷ M concentration (detection limit) of Hg ²⁺ to be the lowest to be detected by 1 .	S7
10. Representative detection limits for Hg ²⁺ reported by various research groups.	S7
11. Emission behavior of 1 in the presence of Hg ²⁺ and other cations.	S8
12. Optimized structure of the putative Hg ²⁺ complex of 1 .	S8
13. Changes in the emission spectrum of 1 , upon sequential addition of Hg ²⁺ and cysteine to the solution of 1 .	S9
14. Cartesian coordinates of the optimized structure of 1 .	S9
15. Cartesian coordinates of the optimized structure of 1 +Hg ²⁺ .	S12
16. Complete reference 20.	S15

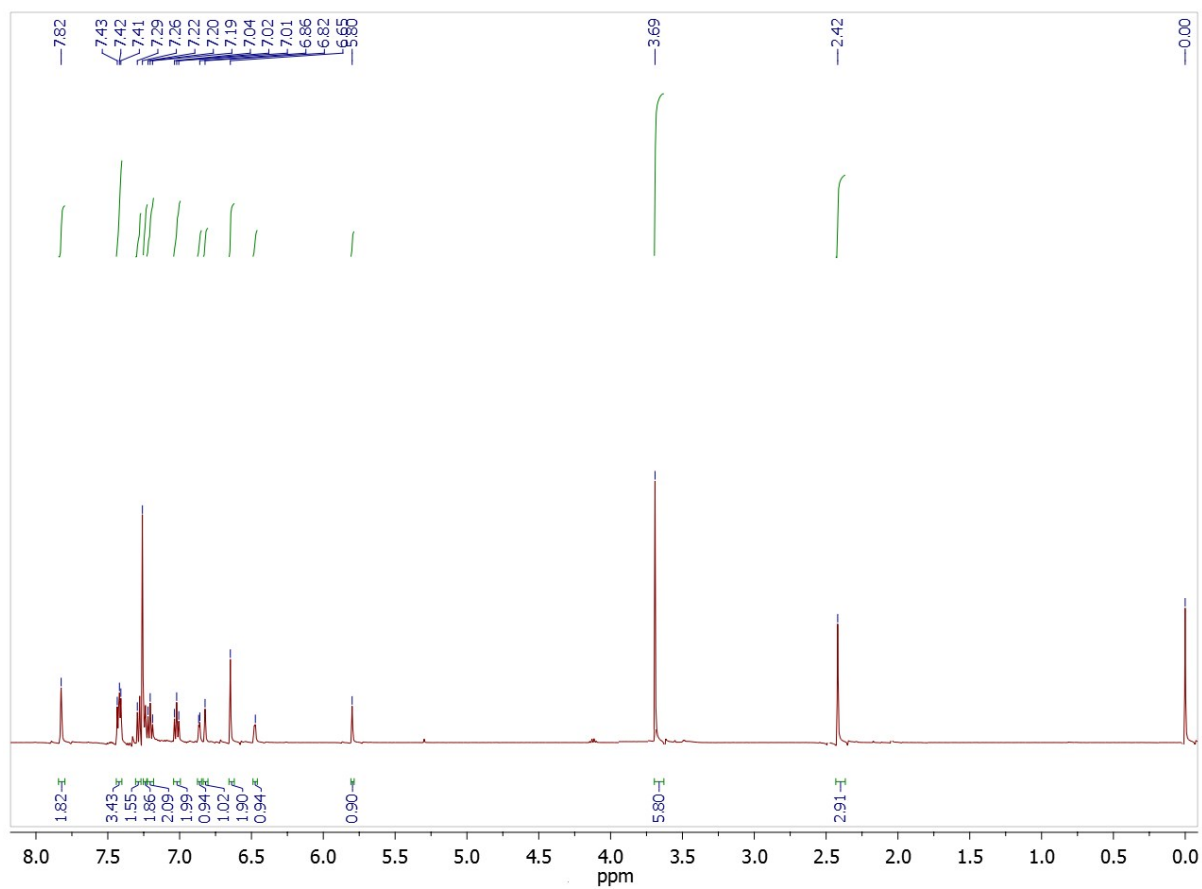


Fig. S1. ^1H NMR spectrum of **1** in CDCl_3 .

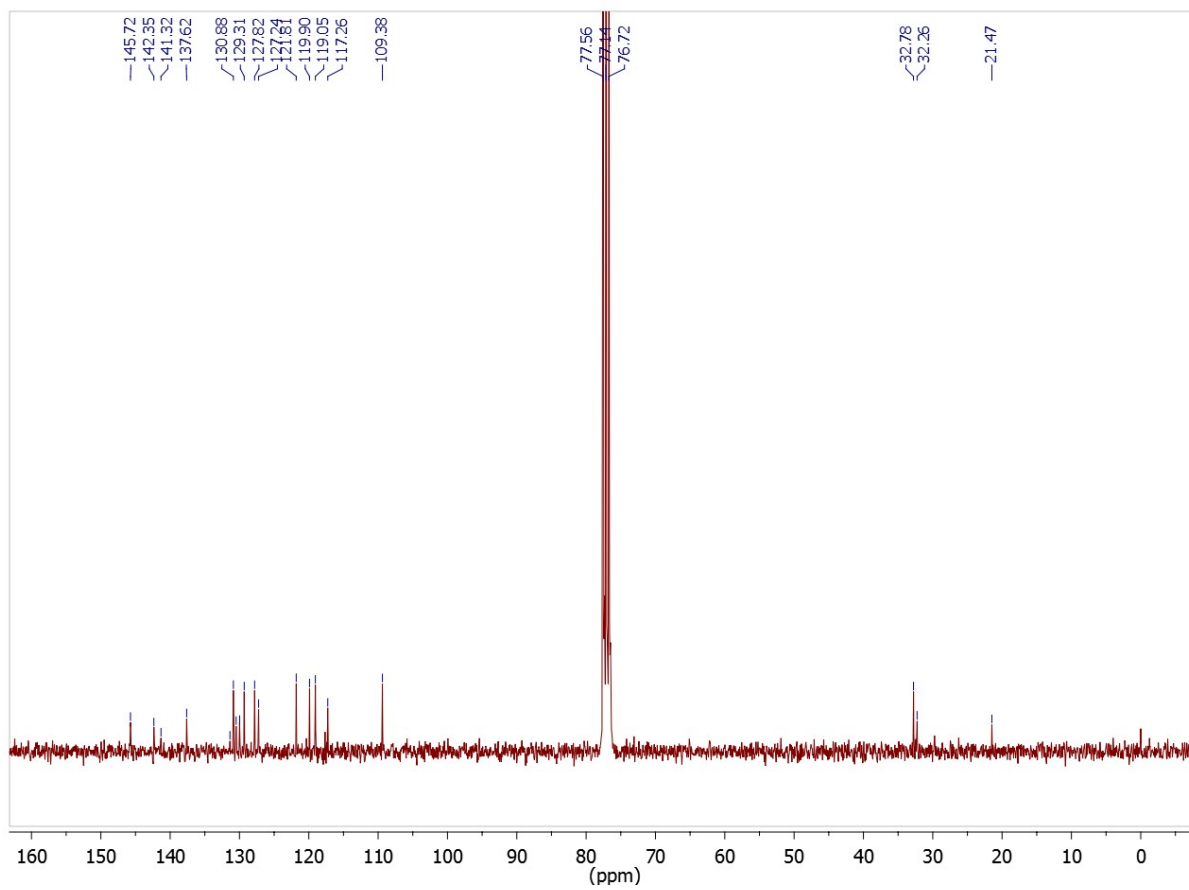


Fig. S2. ^{13}C NMR spectrum of **1** in CDCl_3 .

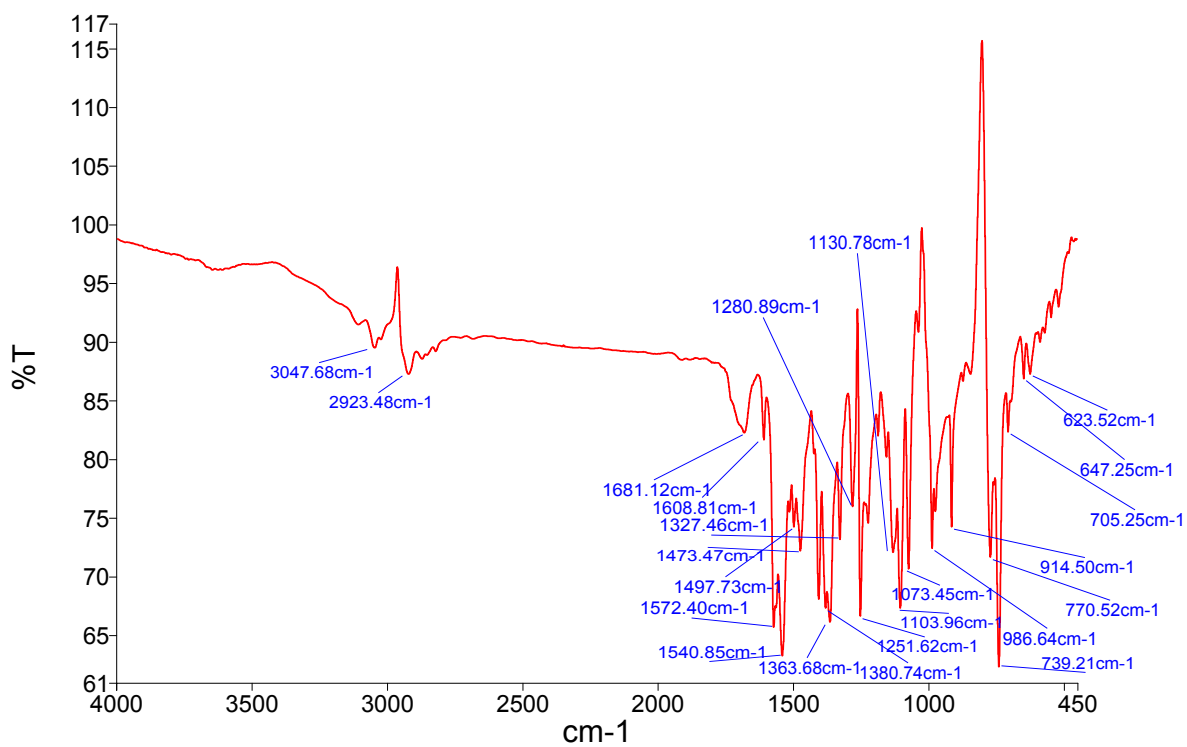


Fig. S3. IR spectrum of **1**.

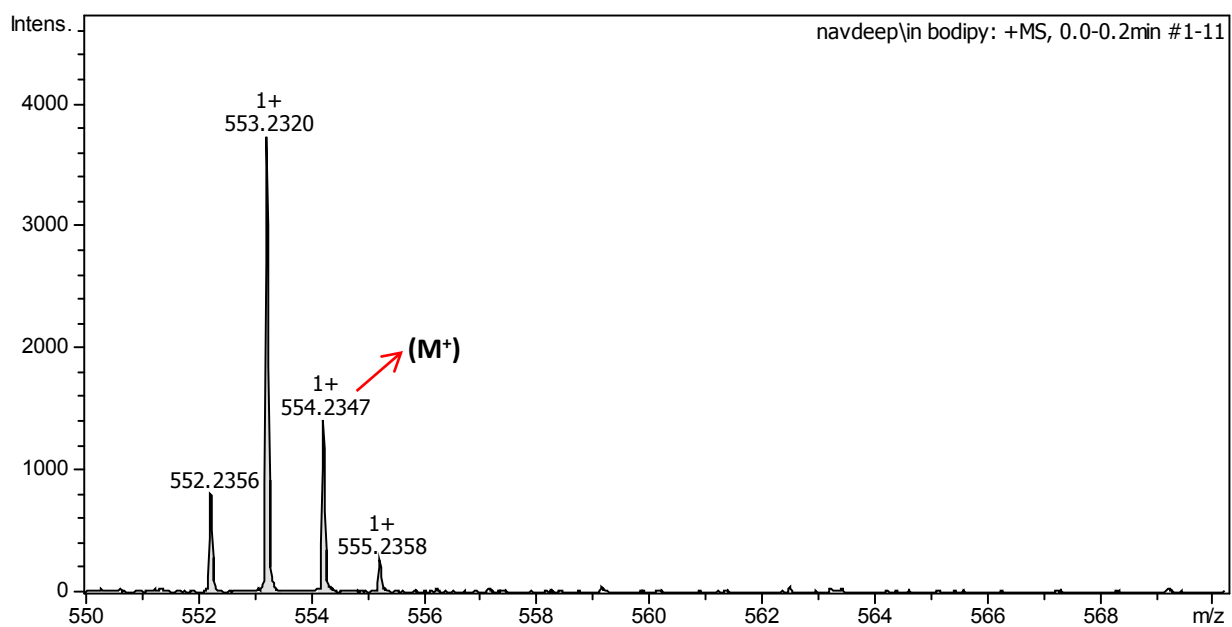


Fig. S4. Mass spectrum of **1**.

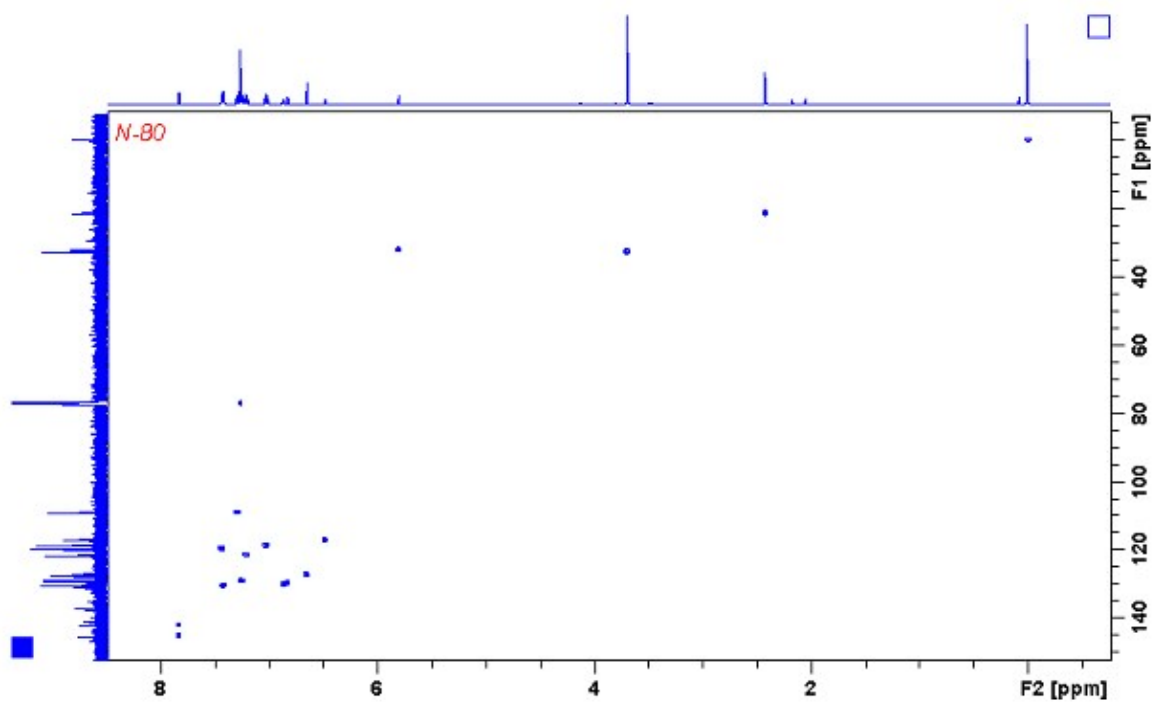


Fig. S5. HSQC spectrum of **1** in CDCl_3 .

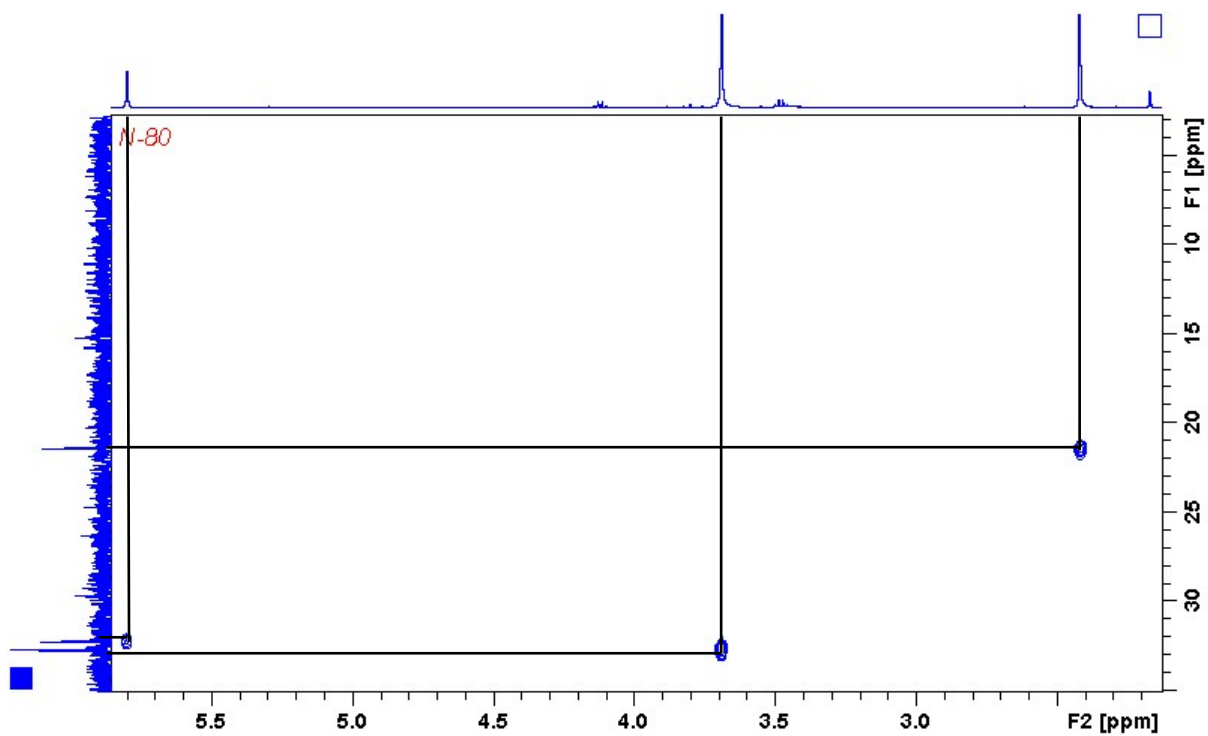


Fig. S5a. Expanded HSQC spectrum of **1**(0-5.8ppm).

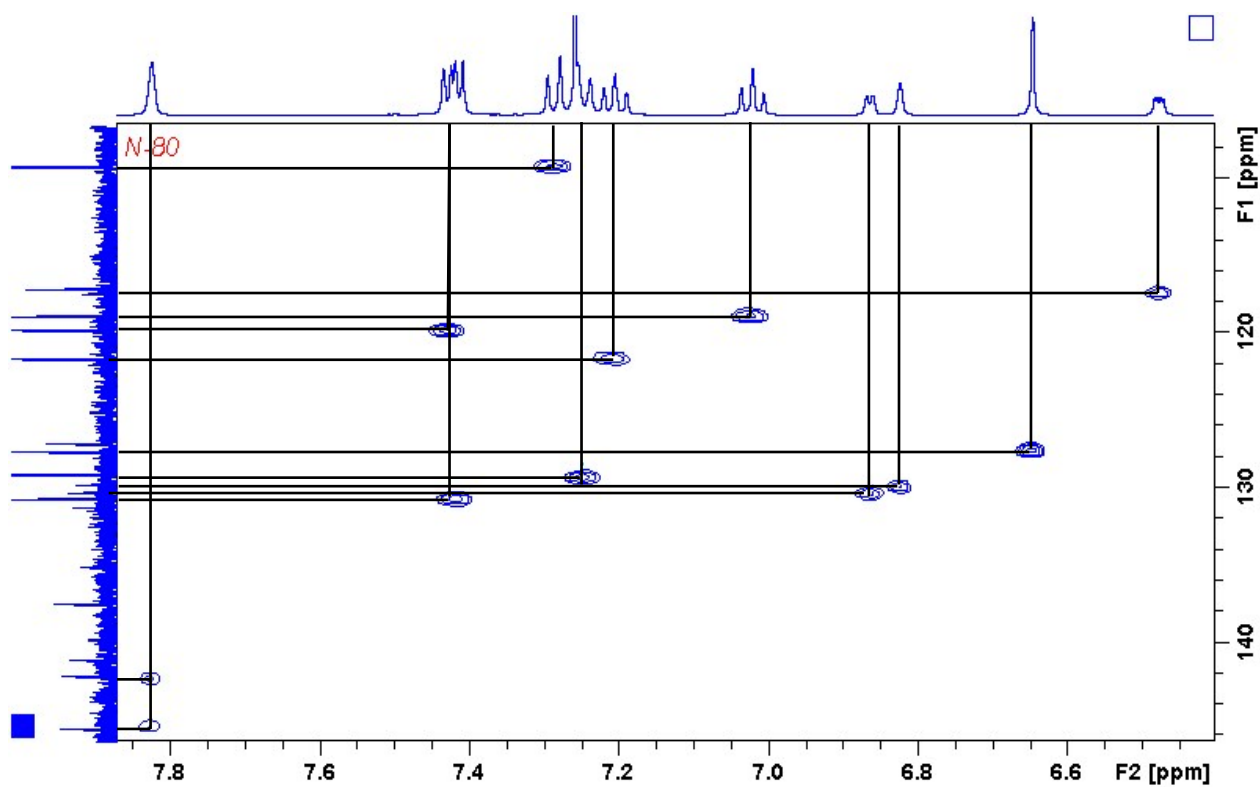


Fig. S5b. Expanded HSQC spectrum of **1** (6 -7.8ppm).

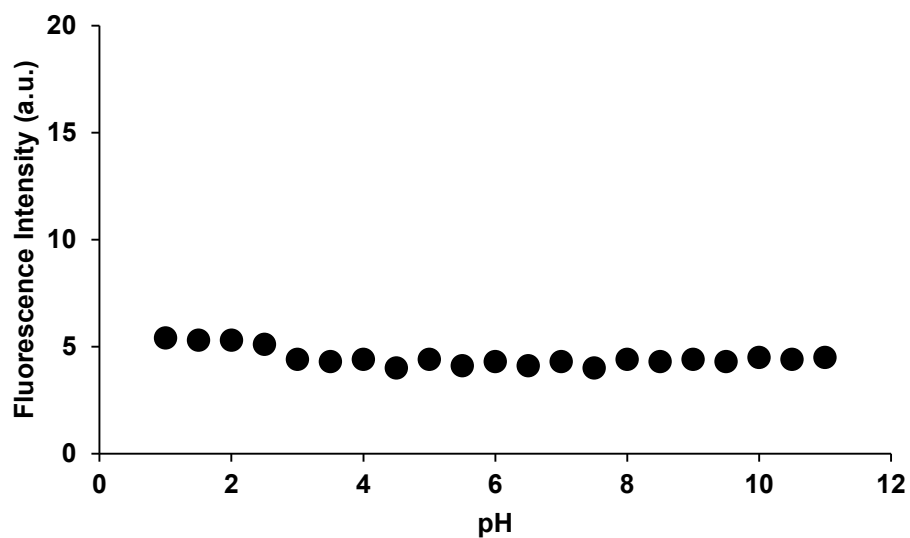


Fig. S6. The emission spectral pattern of **1** (5×10^{-6} M, in CH_3CN) upon pH titrations with HCl (0.01 M) and NaOH (0.01 M) in CH_3CN at 610 nm.

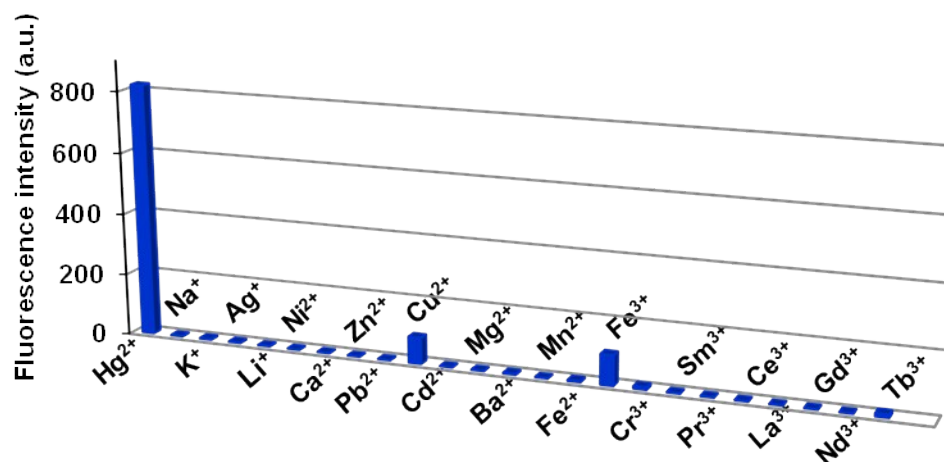


Fig. S7. Changes in the emission behavior of **1** (5.0×10^{-6} M, in CH₃CN) at 610 nm upon addition of various metal ions (3.33×10^{-5} M, in water).

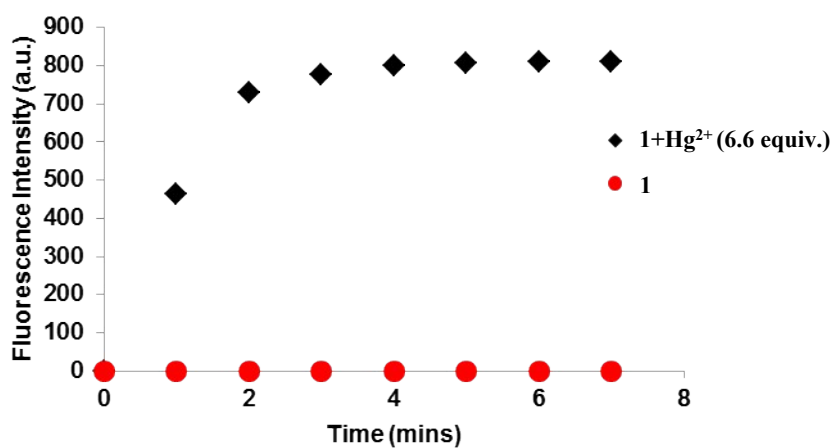


Fig. S8. Responsiveness of **1** in the presence of 6.6 equiv. of Hg²⁺.

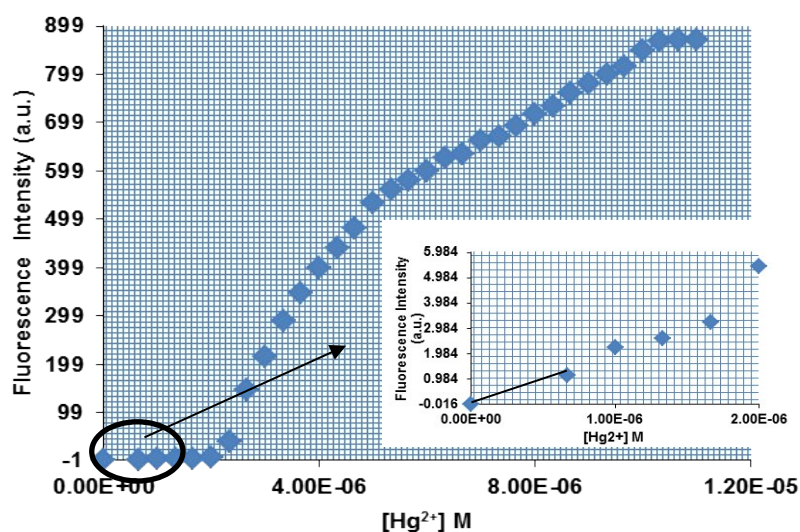


Fig. S9. Increase in the emission intensity at 612 nm of **1** (5×10^{-6} M, in CH_3CN) upon addition of increasing amount of Hg^{2+} (1.7×10^{-7} M to 3.3×10^{-5} M, in H_2O) in CH_3CN . Inset: Graph depicting 3.3×10^{-7} M concentration (detection limit) of Hg^{2+} to be the lowest to be detected by **1**.

Table S1. Representative detection limits for Hg^{2+} reported by various research groups.

References	Detection limit
New J. Chem., 2011 , 35, 1194–1197	0.5×10^{-6} M
Org. Biomol. Chem., 2012 , 10, 5410	0.226×10^{-6} M ,
J. Mater. Chem., 2012 , 22, 11475	0.015×10^{-6} M
Inorg. Chem. 2013 , 52, 11136-11145	0.77×10^{-6} M
Analyst, 2013 , 138, 3809	0.2×10^{-7} M
New J. Chem., 2014 , 38, 3770	0.168×10^{-6} M ,
Chem. Commun., 2014 , 50, 1119	0.65×10^{-7} M,
RSC Adv., 2015 , 5, 30522	1.60×10^{-7} M.
Dalton Trans., 2016 , 45, 2700	0.051×10^{-7} M and 0.072×10^{-7} M
Present work	3.3×10^{-7} M

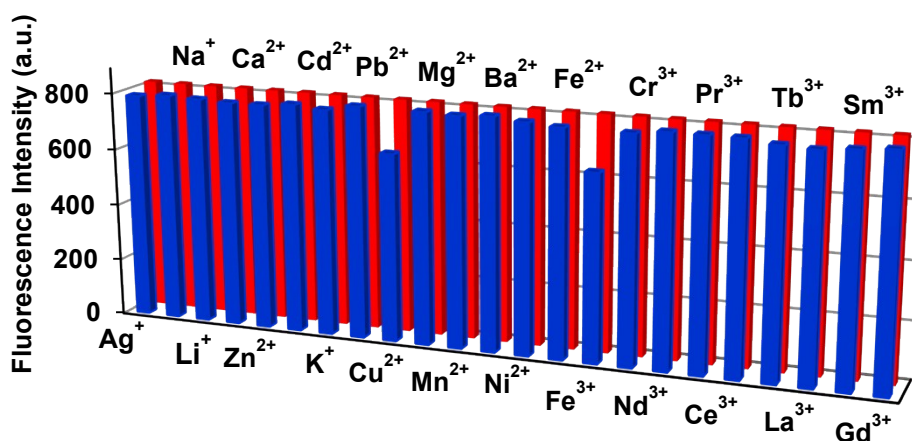


Fig. S10. Emission behavior of **1** (5.0×10^{-6} M, in CH_3CN) in the presence of Hg^{2+} (3.33×10^{-5} M, in water) (red), and Hg^{2+} (3.33×10^{-5} M, in water) in the presence of other cations (3.33×10^{-5} M, in water).

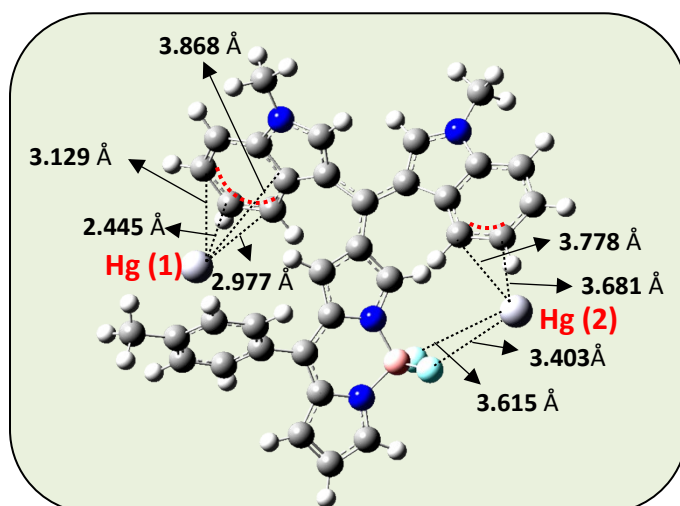


Fig. S11. Optimized structure of the putative Hg^{2+} complex of **1**.

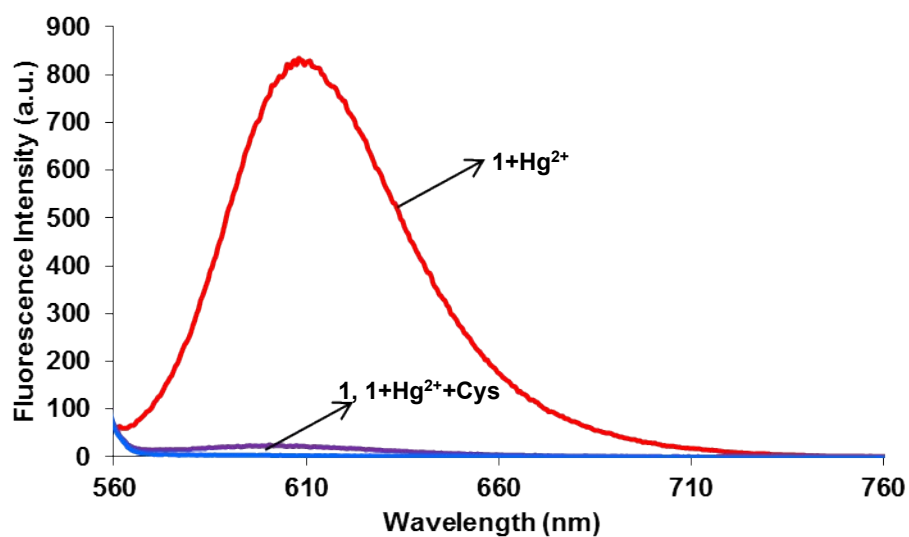


Fig. S12. Changes in the emission spectrum of **1**, upon sequential addition of Hg^{2+} (3.33×10^{-5} M, in water) and cysteine (8.33×10^{-5} M, in water) into solution of **1** (5×10^{-6} M, in CH_3CN).

Table S2. Cartesian coordinates of the optimized structure of **1**.

SCF Done: E(UB3LYP) = -1793.87490205 a.u.

Center Number	Atomic Number	Coordinates (Angstroms)		
		X	Y	Z
1	6	-5.293001	2.389865	1.524048
2	6	-5.668732	1.689710	0.365056
3	6	-4.134244	1.969311	2.199235
4	6	-4.915421	0.613396	-0.106543
5	1	-6.559936	1.994670	-0.176528
6	6	-3.371760	0.898492	1.730253
7	1	-3.830838	2.481904	3.108010

8	6	-3.747772	0.197480	0.565981
9	1	-5.217484	0.098043	-1.011654
10	1	-2.494940	0.579156	2.282859
11	6	-2.950746	-0.945411	0.063082
12	6	-4.931345	-2.602425	-0.064150
13	6	-5.009833	-3.939946	-0.486110
14	1	-5.726672	-2.007664	0.356064
15	6	-3.728865	-4.315672	-0.915659
16	1	-5.883600	-4.573094	-0.472125
17	1	-3.376836	-5.260201	-1.298565
18	6	-3.592427	-2.171849	-0.252913
19	7	-2.875000	-3.259565	-0.776049
20	6	-0.644011	0.226442	0.151921
21	6	0.494570	-1.589911	-0.611786
22	6	0.667103	-0.239031	-0.159925
23	1	-0.898329	1.205377	0.520375
24	1	1.240034	-2.276043	-0.980981
25	6	-1.553551	-0.825954	-0.090630
26	7	-0.796552	-1.927186	-0.581526
27	5	-1.389731	-3.252017	-1.155058
28	9	-1.210019	-3.263589	-2.575282
29	9	-0.703912	-4.368254	-0.588295
30	6	1.919128	0.446373	-0.090602
31	6	0.091549	2.754115	-1.757016
32	6	1.144495	2.861066	-0.829543
33	6	-0.456695	3.916491	-2.298780
34	6	1.633638	4.160211	-0.506006

35	6	1.981082	1.897386	-0.112919
36	6	0.029595	5.192446	-1.942462
37	1	-1.272932	3.839020	-3.009487
38	6	1.087064	5.331204	-1.043945
39	6	2.918189	2.659297	0.586410
40	1	-0.420879	6.077931	-2.379107
41	1	1.472665	6.310880	-0.781662
42	1	3.692237	2.321546	1.257127
43	6	2.710910	-2.384773	1.583147
44	6	3.454298	-1.535936	0.741874
45	6	3.334939	-3.492359	2.155103
46	6	4.834469	-1.826005	0.535715
47	6	3.166280	-0.292070	0.024388
48	6	4.697083	-3.772187	1.912838
49	1	2.761559	-4.155282	2.794241
50	6	5.467384	-2.938560	1.103563
51	6	4.373710	0.095110	-0.558366
52	1	5.151672	-4.647367	2.365439
53	1	6.517398	-3.146171	0.926310
54	1	4.571232	0.942860	-1.195135
55	7	5.369277	-0.817444	-0.268820
56	7	2.711689	4.007338	0.369230
57	6	3.476183	5.098077	0.958809
58	1	3.954536	5.704544	0.181478
59	1	2.830147	5.746152	1.561181
60	1	4.252251	4.682580	1.604172
61	6	6.744030	-0.766428	-0.748211

62	1	7.448301	-0.747814	0.090929
63	1	6.971168	-1.633811	-1.377900
64	1	6.882384	0.140051	-1.340255
65	6	-6.095849	3.572952	2.016359
66	1	-5.709039	4.515311	1.604218
67	1	-7.146946	3.495496	1.718867
68	1	-6.057915	3.656933	3.107899
69	1	-0.293759	1.783612	-2.043391
70	1	1.663982	-2.189415	1.781957

Table S3. Cartesian coordinates of the optimized structure of **1**+Hg²⁺.

SCF Done: E(UB3LYP) = -2100.80572668 a.u.

Center Number	Atomic Number	Coordinates (Angstroms)		
		X	Y	Z
1	6	-5.134416	-2.111179	2.420757
2	6	-4.961079	-2.780384	1.198033
3	6	-3.993072	-1.603444	3.060026
4	6	-3.692866	-2.951564	0.638905
5	1	-5.827098	-3.183881	0.679926
6	6	-2.725453	-1.748771	2.501682
7	1	-4.096833	-1.089222	4.011846
8	6	-2.553805	-2.429797	1.282616
9	1	-3.588868	-3.464577	-0.311976
10	1	-1.859507	-1.359550	3.027787
11	6	-1.210278	-2.577786	0.686406
12	6	-1.325470	-5.120217	0.338030

13	6	-0.432360	-6.010042	-0.229798
14	1	-2.292418	-5.345735	0.763471
15	6	0.700672	-5.257804	-0.618783
16	1	-0.552216	-7.076857	-0.354016
17	1	1.617285	-5.604635	-1.077606
18	6	-0.734568	-3.821577	0.271301
19	7	0.528590	-3.962825	-0.324559
20	6	-0.678181	-0.067507	0.693771
21	6	1.392191	-0.298180	-0.189353
22	6	0.460118	0.666784	0.277189
23	1	-1.588618	0.338515	1.107221
24	1	2.367514	-0.143784	-0.629759
25	6	-0.398155	-1.421160	0.496632
26	7	0.884501	-1.523543	-0.061073
27	5	1.618366	-2.856322	-0.417002
28	9	2.156406	-2.785045	-1.694270
29	9	2.624137	-3.096123	0.521313
30	6	0.633856	2.097322	0.286136
31	6	-2.185464	1.869318	-1.531906
32	6	-1.767710	2.759690	-0.549990
33	6	-3.482000	2.034096	-2.107040
34	6	-2.612307	3.862224	-0.220242
35	6	-0.534395	2.942929	0.200257
36	6	-4.314886	3.140370	-1.721220
37	1	-3.683931	1.547789	-3.061927
38	6	-3.887283	4.055523	-0.781998
39	6	-0.707925	4.124231	0.914661

40	1	-5.274404	3.266999	-2.210461
41	1	-4.500338	4.907906	-0.511622
42	1	-0.043706	4.582472	1.633513
43	6	3.536321	1.094389	1.741807
44	6	3.160290	2.214859	0.987122
45	6	4.844978	1.010622	2.218608
46	6	4.115971	3.236174	0.776851
47	6	1.907991	2.696288	0.399184
48	6	5.784081	2.026272	1.962989
49	1	5.139786	0.147639	2.807817
50	6	5.428789	3.164317	1.240732
51	6	2.207681	3.981216	-0.122080
52	1	6.794936	1.932009	2.347169
53	1	6.140755	3.963286	1.063497
54	1	1.566189	4.639290	-0.690165
55	7	3.492730	4.284112	0.078626
56	7	-1.940923	4.658564	0.678021
57	6	-2.467051	5.882146	1.284238
58	1	-2.655005	6.630005	0.509784
59	1	-3.394306	5.663542	1.818901
60	1	-1.728368	6.268333	1.985709
61	6	4.172086	5.493220	-0.379967
62	1	4.595956	6.022997	0.476751
63	1	4.971855	5.226340	-1.075463
64	1	3.449662	6.135835	-0.882616
65	6	-6.500880	-1.973993	3.045879
66	1	-7.290663	-1.981409	2.288358

67	1	-6.697628	-2.808160	3.732214
68	1	-6.584060	-1.049727	3.626291
69	1	-1.540790	1.075339	-1.891749
70	1	2.828165	0.305142	1.966787
71	80	5.268909	-1.286727	-0.626377
72	80	-4.524120	0.091734	-1.047795

Complete reference 20

Gaussian 09, Revision B.01, Frisch, M. J.; Trucks, G. W.; Schlegel, H. B.; Scuseria, G. E.; Robb, M. A.; Cheeseman, J. R.; Scalmani, G.; Barone, V.; Mennucci, B.; Petersson, G. A.; Nakatsuji, H.; Caricato, M.; Li, X.; Hratchian, H. P.; Izmaylov, A. F.; Bloino, J.; Zheng, G.; Sonnenberg, J. L.; Hada, M.; Ehara, M.; Toyota, K.; Fukuda, R.; Hasegawa, J.; Ishida, M.; Nakajima, T.; Honda, Y.; Kitao, O.; Nakai, H.; Vreven, T.; Montgomery, J. A., Jr.; Peralta, J. E.; Ogliaro, F.; Bearpark, M.; Heyd, J. J.; Brothers, E.; Kudin, K. N.; Staroverov, V. N.; Keith, T.; Kobayashi, R.; Normand, J.; Raghavachari, K.; Rendell, A.; Burant, J. C.; Iyengar, S. S.; Tomasi, J.; Cossi, M.; Rega, N.; Millam, J. M.; Klene, M.; Knox, J. E.; Cross, J. B.; Bakken, V.; Adamo, C.; Jaramillo, J.; Gomperts, R.; Stratmann, R. E.; Yazyev, O.; Austin, A. J.; Cammi, R.; Pomelli, C.; Ochterski, J. W.; Martin, R. L.; Morokuma, K.; Zakrzewski, V. G.; Voth, G. A.; Salvador, P.; Dannenberg, J. J.; Dapprich, S.; Daniels, A. D.; Farkas, O.; Foresman, J. B.; Ortiz, J. V.; Cioslowski, J.; Fox, D. J. Gaussian, Inc., Wallingford CT, 2010.